Electronic Supplementary Information (ESI) For

Tetraphenylethylene (TPE)-based supra-amphiphilic organoplatinum(II) metallacycle and its self-assembly behaviour

Wei Zheng,[‡, a] Guang Yang,[‡, b] Shu-Ting Jiang,[a] Nannan Shao,[c] Guang-Qiang Yin,[a,d] Lin Xu,[a] Xiaopeng Li,[d] Guosong Chen*[,b] and Hai-Bo Yang*[,a]

[a] Shanghai Key Laboratory of Green Chemistry and Chemical Processes, Department of Chemistry, East China Normal University, Shanghai 200062, P. R. China.

[b] The State Key Laboratory of Molecular Engineering of Polymers and Department of Macromolecular Science, Fudan University, Shanghai 200433, P. R. China.

[c] State Key Laboratory of Polymer Physics and Chemistry, Changchun Institute of Applied Chemistry Chinese Academy of Science Changchun 130022, P. R. China

[d] Department of Chemistry, University of South Florida, Tampa, Florida 33620, United States

E-mail: hbyang@chem.ecnu.edu.cn.
guosong@fudan.edu.cn

Table of Contents

1. General Information.

All reagents were of analytical purity and used without further treatment. *N*-isopropylacrylamide (NIPAAM was recrystallized twice from hexane prior to use) and azodiisobutyronitrile (AIBN was recrystallized from ethanol before use) were purchased from Energy Chemical Reagent Co. 2-Methyl-2-[(dodecylsulfanylthiocarbony) sulfanyl] propanic acid was purchased from *J&K Co*. TLC analysis was performed on silica-gel plates, and flash chromatography was conducted by using silica-gel column packages. All solvents were dried according to the standard procedures and all of them were degassed under N_2 for 30 minutes before use. All air-sensitive reactions were carried out under argon atmosphere. ^{1}H NMR and ^{31}P NMR spectra were recorded on Bruker 400 MHz Spectrometer (^{1}H: 400 MHz; ^{31}P: 161.9 MHz) at 298 K. The ^{1}H NMR chemical shifts are reported relative to the residual solvent signals, and ^{31}P NMR resonances are referenced to an internal standard sample of 85% H_3PO_4 (δ 0.0). Coupling constants (J) are denoted in Hz and chemical shifts (δ) in ppm. Multiplicities are denoted as follows: s = singlet, d = doublet, m = multiplet, br = broad. TEM images were recorded on a Tecnai G^2 F30 (FEI Ltd.). The sample for TEM measurements was prepared by dropping the solution onto a carbon-coated copper grid. DLS measurements were performed under a Malvern Zetasizer Nano-ZS light scattering apparatus (Malvern Instruments, U.K.) with a He-Ne laser (633 nm, 4 mW). Gel permeation chromatography (GPC) analysis was carried out with a Waters Breeze 1515 GPC analysis system with TOSOH TSK gel α-3000 and α-2500 columns in series, using DMF with 0.5 M LiBr as eluent at the flow rate of 1 mL/min at 80℃. PEG calibration kit (purchased from TOSOH) was used as the calibration standard. Confocal laser scanning microscopy (CLSM) imaging was performed with an OLYMPUS ZX81 laser scanning microscope and a 60x oil-immersion objective lens. A 405nm laser was selected as the excitation source. Quantum yields were determined using quinine sulfate at 365 nm (ΦF = 56%).

2. Synthesis and Characterization of New Compounds.

Scheme S1. Synthesis route of complex **c**.

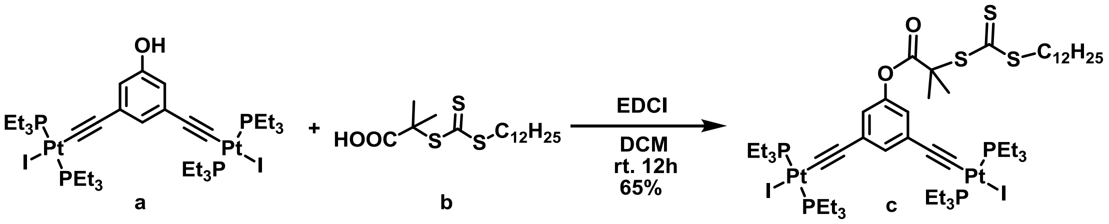

Synthesis of c. A 200 mL Schlenk flask was charged with **a** [S1] (1.0 g, 0.796 mmol), **b** (435 mg, 1.19 mmol), and EDCI (1.216 g, 6.36 mmol), degassed, and back-filled three times with N_2. Anhydrous dichloromethane (30.0 mL) was introduced into the reaction flask by syringe. The reaction was stirred under an inert atmosphere at 0℃ for 2.0 min and 12 h at room temperature. The solvent was then removed under reduced pressure. The residue was purified by column chromatography on silica gel (Petroleum ether/ethyl acetate = 4/1) to give product as a pale yellow solid. Yield: 830 mg, 65%. R_f = 0.30 (Petroleum ether /ethyl acetate = 2:1). Mp: 76-77 ºC. ^{1}H NMR ($CDCl_3$, 400 MHz): δ 7.02 (s, 1 H), 6.78 (s, 2H), 3.26-3.29 (t, 2 H, J = 6 Hz), 2.19-2.22 (m, 24 H), 1.66-1.68 (m, 3 H), 0.88-1.57 (m, 54H), 0.86-0.88 (t, 3H, J = 5.2Hz); ^{13}C NMR ($CDCl_3$, 100 MHz): δ 171.56, 150.58, 130.54, 129.29, 120.90, 99.46, 90.87, 90.76, 90.64, 55.79, 37.09, 32.92, 29.65, 29.63, 29.57, 29.50, 29.35, 29.13, 29.05, 27.83, 25.32, 22.70, 16.78, 16.64, 16.50, 14.14, 8.32. ^{31}P NMR (acetone-d_6, 161.9 MHz): δ 8.84 (s, $J_{\text{Pt-P}}$ = 1937.9 Hz); MS (ESI) m/z 674.23 ($[M-2I^-]^{2+}$)

Scheme S2. Synthesis route of 120° CTA-based di-Pt(II) acceptor **2**.

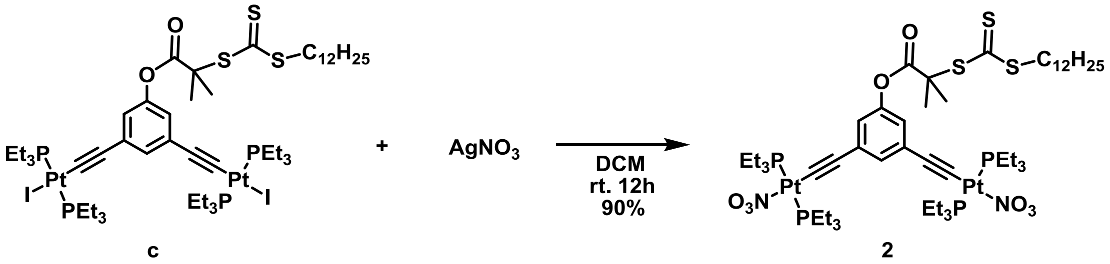

Synthesis of 120° CTA-based di-Pt(II) acceptor 2. A 50 mL round-bottom Schlenk flask was charged with 200 mg (0.125 mmol) of **c** and 10 mL of dichloromethane. To the solution was added 47.68 mg (0.28 mmol) of $AgNO_3$ at once, resulting in a yellowish precipitate of AgI. After 12 h at room temperature, the suspension was filtered through a glass fiber filter and the volume of the solution reduced to 5.0 mL. Subsequent addition of diethylether resulted in the precipitation of the bistriflate salt **2** as a slightly yellow powder: yield 165 mg, 90%; mp: 82-83 °C; ^{1}H NMR (acetone-*d6*,, 400 MHz): δ 6.97 (s, 1 H), 6.78 (s, 2H), 3.40-3.43 (t, 2 H, *J* =8 Hz), 2.02-2.06 (m, 27 H), 1.23-2.01 (m, 55 H), 0.86-0.88 (m, 6H); ^{31}P NMR (acetone-d_6, 161.9 MHz): δ 21.48 (s, $J_{\text{Pt-P}}$ = 2059.6Hz); IR (neat): 2923, 2853, 2119, 1753, 1589, 1484, 1143, 1034, 764. MS (ESI) *m*/*z* 674.23 ($[M\text{-}2NO_3^-]^{2+}$)

Scheme S3. Self-assembly of supramolecular metallacycle **3** from 120° TPE containing dipyridyl donor **1** and the 120° CTA-based di-Pt(II) acceptor **2**.

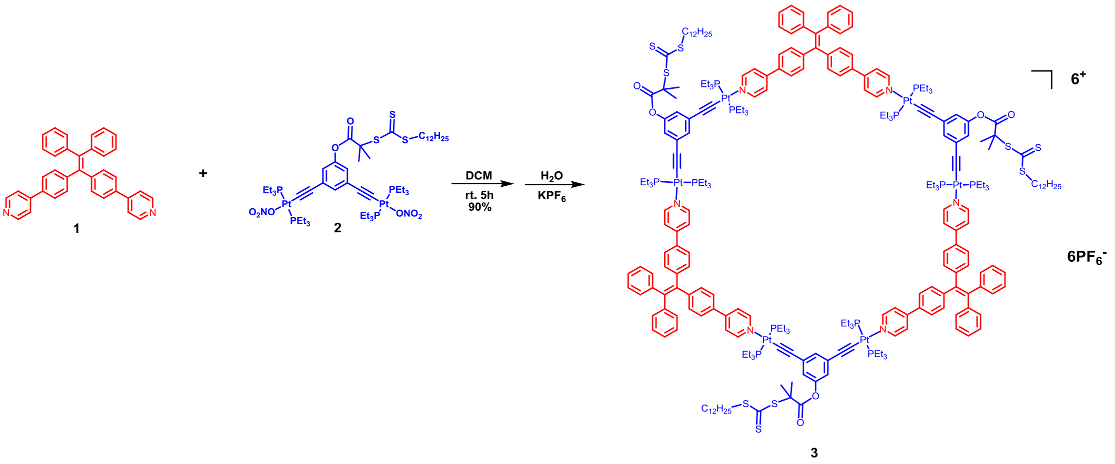

Self-assembly of supramolecular metallacycle 3 from 120° TPE containing dipyridyl donor 1 and the 120° CTA-based di-Pt(II) acceptor 2. The dipyridyl donor ligand **1** (3.11 mg, 6.39 μmol) and the 120° organoplatinum acceptor **2** (9.41 mg, 6.39 μmol) were weighed accurately into a glass vial. To the vial was added 5.0 mL dichloromethane, and the reaction solution was then stirred at room temperature for 5 h to yield a homogeneous yellow solution. Then the addition of a saturated aqueous solution of KPF_6 into the bottle with continuous stirring (10 min) precipitated the product. The reaction mixture was centrifuged, washed several times with water, and dried. Yellow solid product **3** was obtained by removing the solvent under vacuum. Yield: 11.2 mg, 90%. Mp: > 285 ºC, decomposed. ^{1}H NMR (acetone-d_6, 400 MHz): δ 8.92-8.93 (d, 4 H, J = 6 Hz), 8.06-8.07 (d, 4 H, J = 6.4 Hz), 7.81 (s, 4 H), 7.29-7.32 (t, 4 H, J = 5.2 Hz), 7.20 (s, 6 H) 7.12-7.14 (t, 4 H, J = 3.6 Hz), 7.06 (s, 1 H), 6.90 (s, 2 H), 3.40-3.43 (t, 2 H, J = 7.2 Hz), 1.82-196 (m, 35 H), 1.20-1.28 (m, 65 H), 0.86-0.87 (m, 7 H); ^{31}P NMR (acetone-d_6, 161.9 MHz): δ 16.70 (s, $J_{\text{Pt-P}}$ = 2430.0 Hz); IR (neat): 2922, 2851, 2119, 1748, 1612, 1567, 1489, 1330, 1142, 816, 734; ESI-TOF-MS of **4**: calcd for $[M - 6\ PF_6^-]^{6+}$: 918.17, found: 918.06; calcd for $[M - 5\ PF_6^-]^{5+}$: 1130.60, found: 1330.74, calcd for $[M - 4\ PF_6^-]^{4+}$: 1449.74, found: 1449.88.

Scheme S4. Synthesis route of supramolecular star polymer **4**.

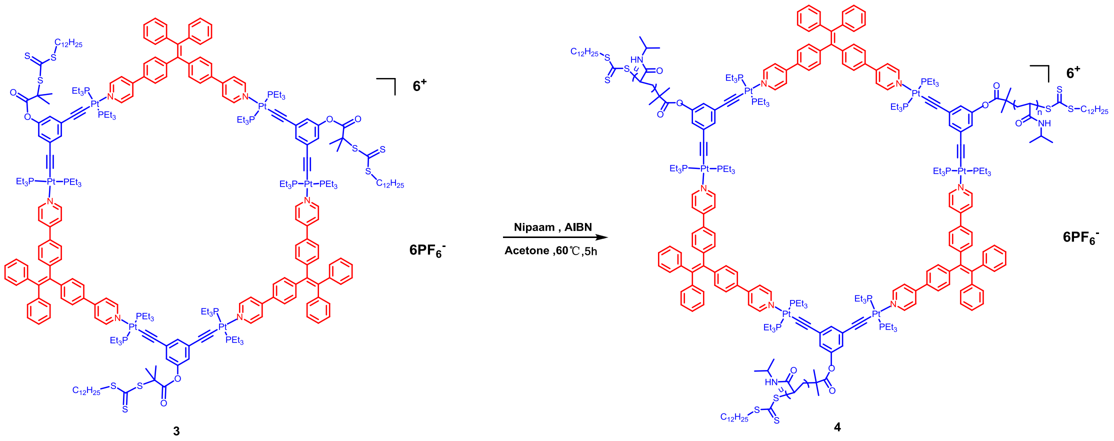

Synthesis of star supramolecular polymer 4. Supramolecular metallacycle **3** (40 mg, 6.1 μmol), AIBN (0.48 mg, 3.0 μmol), *N*-isopropylacrylamide (350 mg, 3.0 mmol), and 1.0 mL of acetone were added in a 10.0 mL flask equipped with a magnetic stirring bar. After being degassed by freeze-pump-thaw cycles for three times, the mixed solution was immediately transferred to the preheated oil bath at 60 ℃ to initiate the polymerization. After 5 h, the polymerization was quenched by liquid N_2, and the resulting mixture was precipitated in diethyl ether. The precipitate was dissolved in acetone and then precipitated again in the presence of diethyl ether. The above dissolution-precipitation cycle was repeated three times. The final product was dried in vacuum, as a yellow solid (210 mg, $M_{\mathrm{n,NMR}}$ = 15 kDa, $M_{\mathrm{n,GPC}}$ = 12 kDa, PDI = 1.20). ^{1}H NMR (acetone-d_6, 400 MHz): 6.98-7.77 (br s, -N*H*), 4.02 (br s, -NC*H*), 1.15-2.04 (br m, backbone), 0.83-0.88(s, -CH_3 end-group) ; ^{31}P NMR (acetone-d_6, 161.9 MHz): δ 17.08 (s, $J_{\mathrm{Pt\text{-}P}}$ = 2436.7 Hz); IR (neat): 3289, 2973, 2367, 1640, 1544,1460, 1387, 1367, 1171,1131 cm^{-1}.

Reference:

S1. K. Ghosh, Y. Zhao, H.-B. Yang, B. H. Northrop, H. S. White and P. J. Stang, *J. Org. Chem.* 2008, **73**, 8553–8557

3. Characterization of Star Supramolecular Polymer 4.

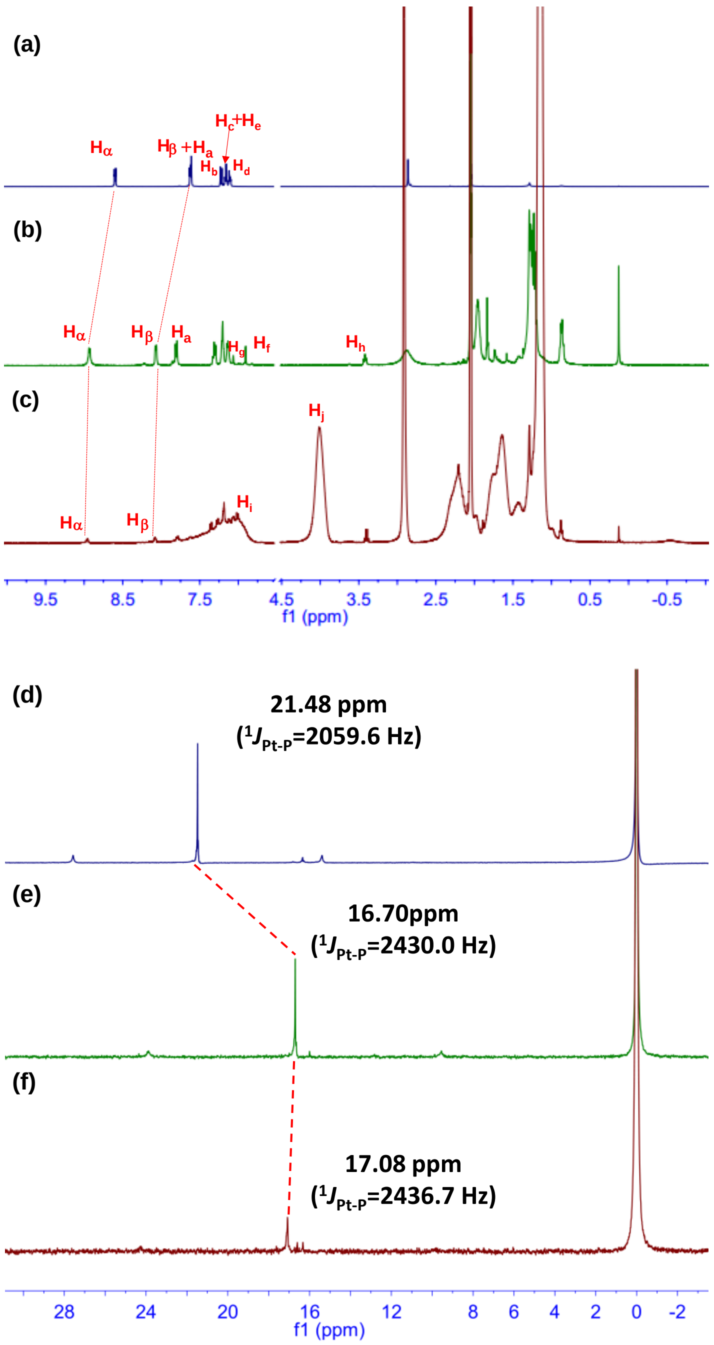

Fig. S1 Partial ^{1}H NMR spectra (400 MHz, 298 K) of 120° TPE-based dipyridyl donor **1** (a), hexagonal metallacycle **3** (b), and star supramolecular polymer **4** (c) in acetone-d_6. ^{31}P {^{1}H} NMR spectra (161.9 MHz, 298 K) of 120° CTA-based di-Pt (II) acceptors **2** (d), hexagonal metallacycle **3** (e), and star supramolecular polymer **4** (f) in acetone-d_6.

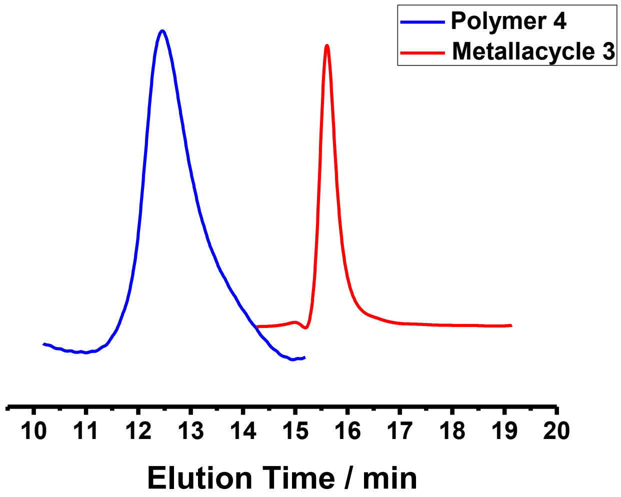

Fig. S2 GPC trace of hexagonal metallacycle **3** (red) and star supramolecular polymer **4** (blue).

4. The Photo Luminescent Property of Star Supramolecular Polymer 4.

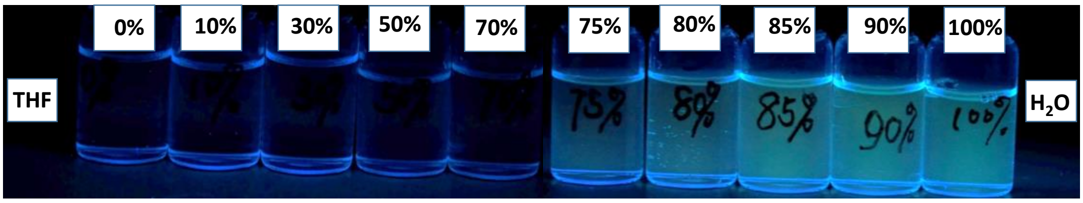

Fig. S3 The photographs of the polymer **4** in THF/H_2O mixtures with different fractions of water on excitation at 365 nm using an ultraviolet lamp at 298 K with the concentration of 1.0 mg/mL.

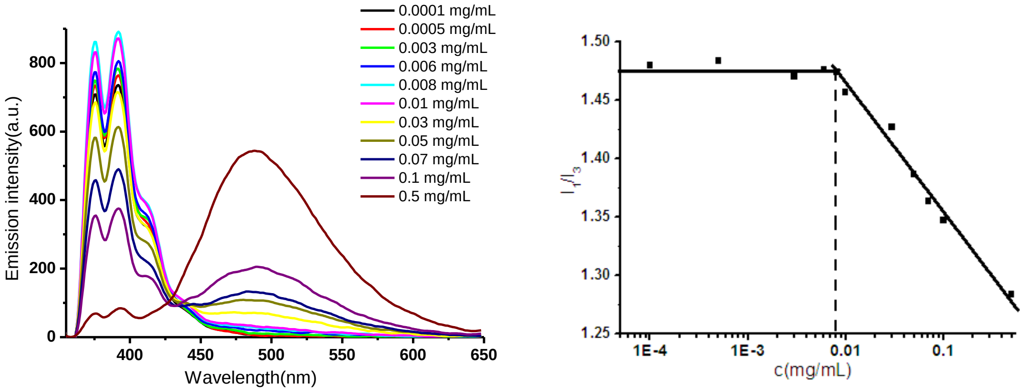

Fig. S4 Determination of CAC for the polymer **4** using the fluorescent method with pyrene as a probe.

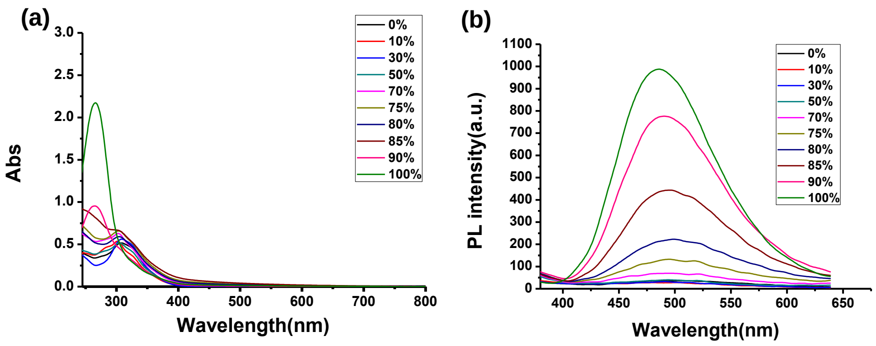

Fig. S5 Absorption (a) and fluorescence emission spectrum (b) of TPE-based star polymer **4** versus the water fraction in the THF/water mixtures

As shown in Fig.S6, the emission of polymer **4** showed a very slight blue shift (*ca.* 8 nm) of the emission maximum. In this study the AIE property of polymer **4** was investigated in THF/water mixed solvent system. We speculate that the polarity of the mixed solvent change slightly with the increase of the water fraction as both THF and H_2O are polar solvents. Thus, no obvious charge-transfer within the assemblies induced by polarity change of solvents occurred, thereby resulting in no obvious shift in the absorption and emission during the aggregation process.

5. AFM Images of TPE-based Star Polymer 4.

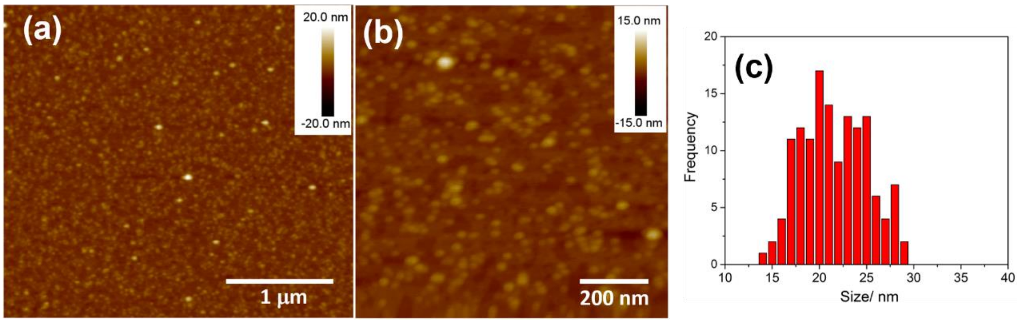

Fig. S6 AFM images of TPE-based star polymer **4** (1.0 mg/mL, aqueous solution) at 25 ℃ ((a) and (b)) and the size distribution of nanoparticles obtained from image b (c).

6. The Cytotoxicity of Star Supramolecular Polymer 4.

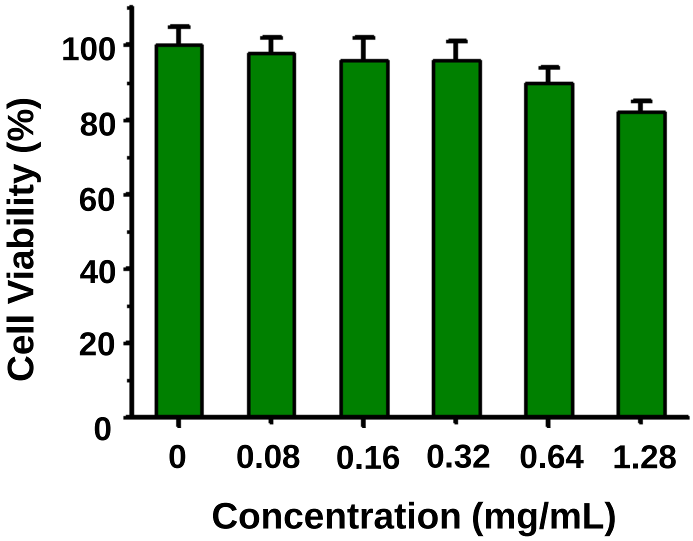

Fig. S7 Cell viability of BMSCs treated with different concentration of polymer **4**.

7. ^{1}H, ^{31}P, ^{13}C NMR, IR and MS Spectra of New Compounds

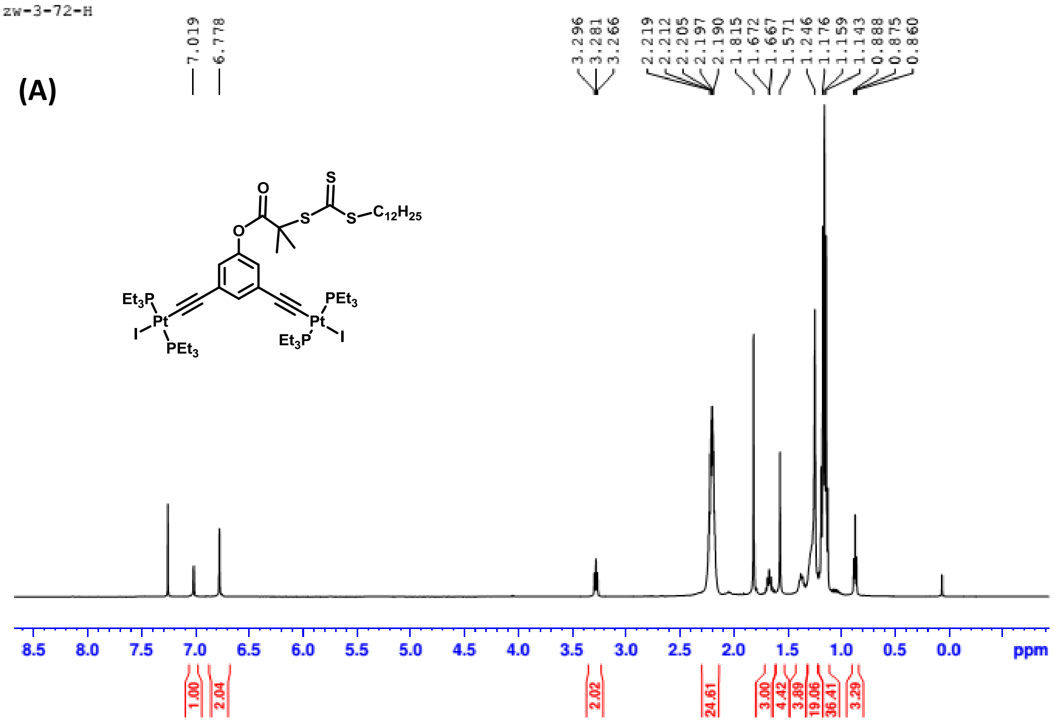

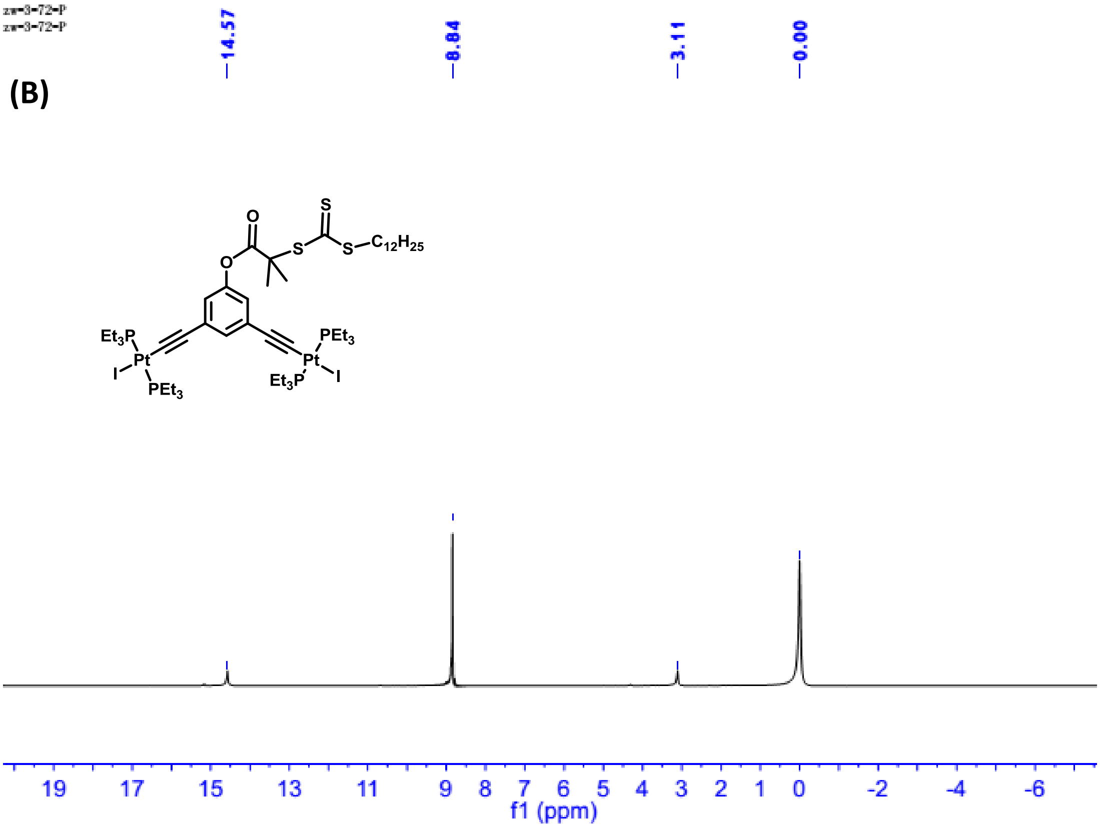

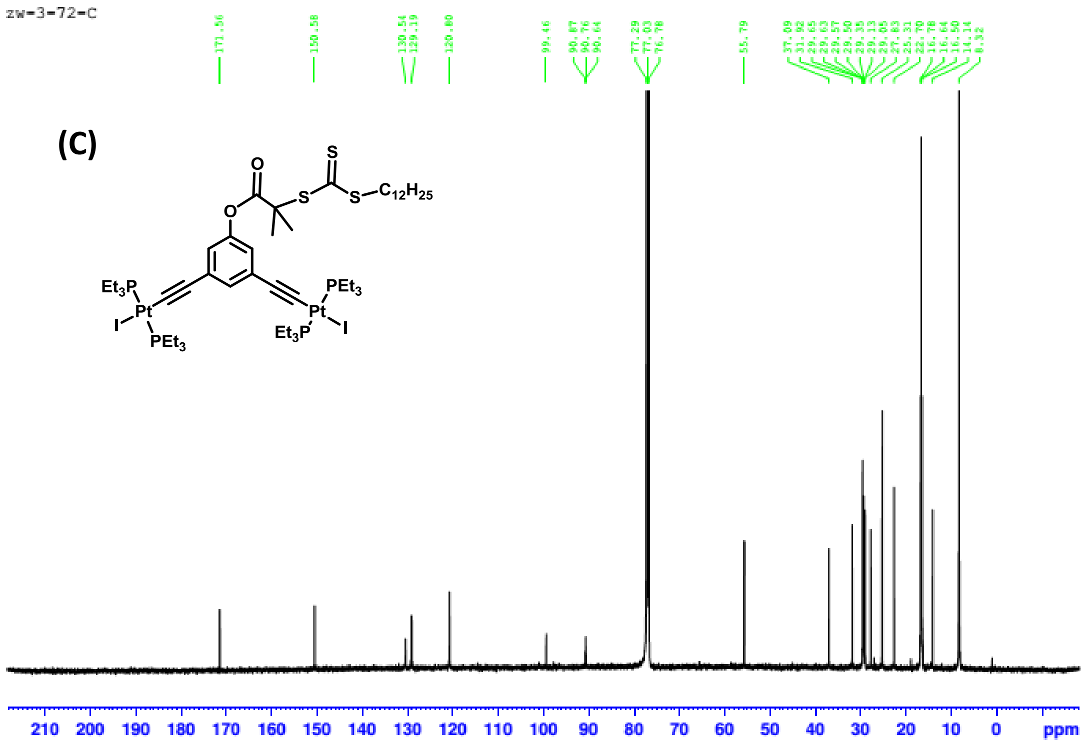

Fig. S8 (A) ^{1}H NMR spectra of **c** in $CDCl_3$, (B) ^{31}P NMR spectra of **c** in $CDCl_3$, (C) ^{13}C NMR spectra of **c** in $CDCl_3$

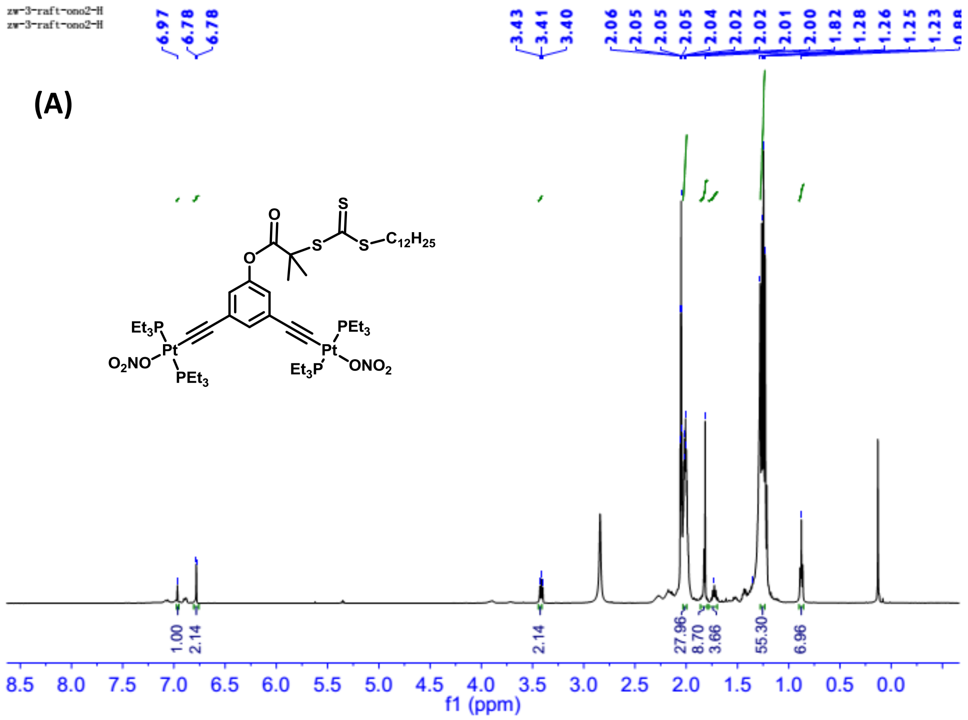

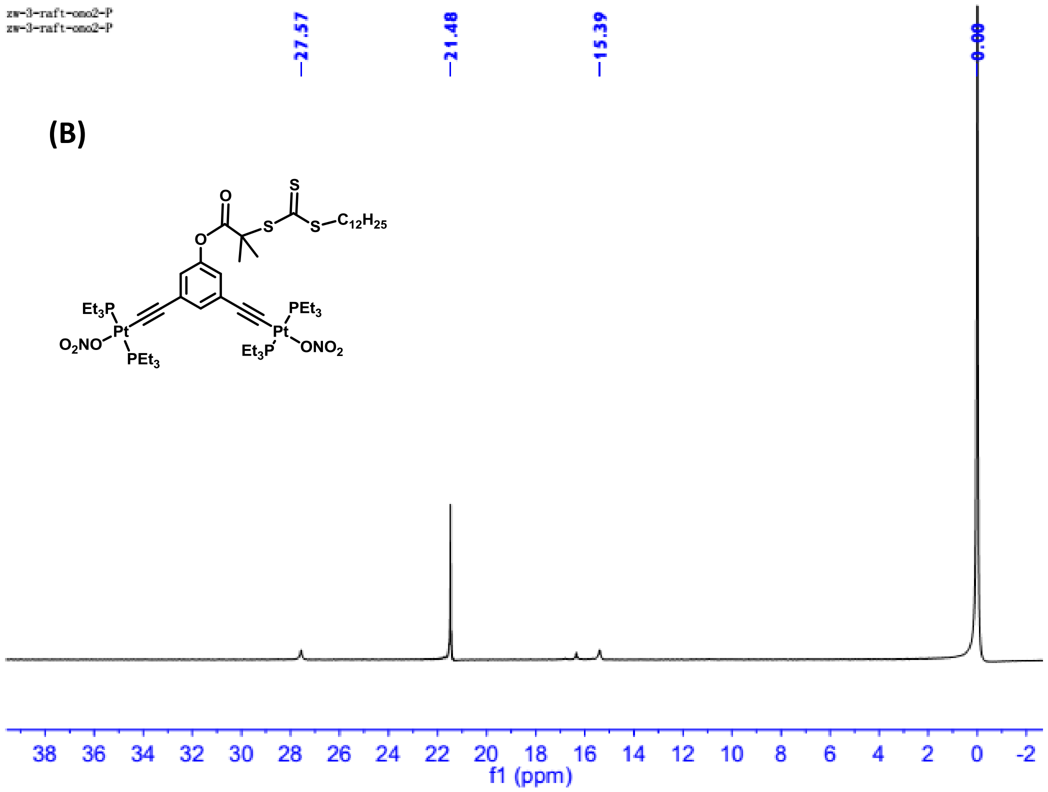

Fig. S9 (A) ^{1}H and (B) ^{31}P NMR spectra of **2** in acetone-d_{6}.

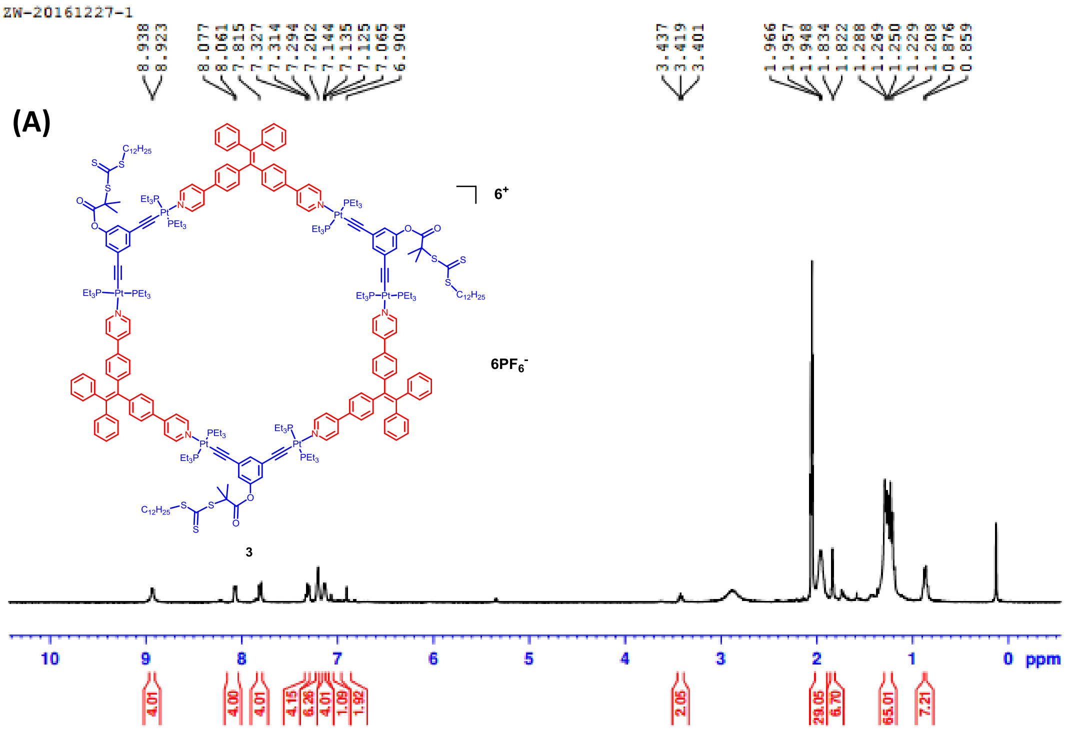

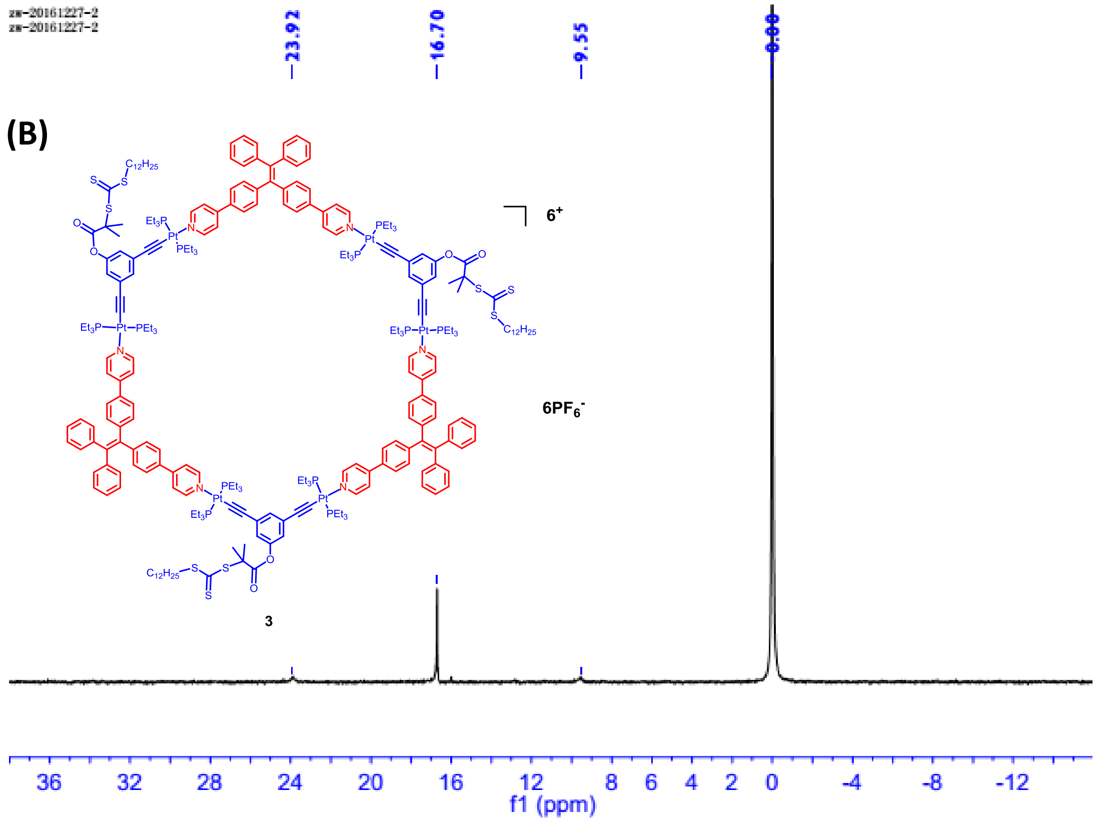

Fig. S10 (A) ^{1}H and (B) ^{31}P NMR spectra of metallacycle **3** in acetone-d_6.

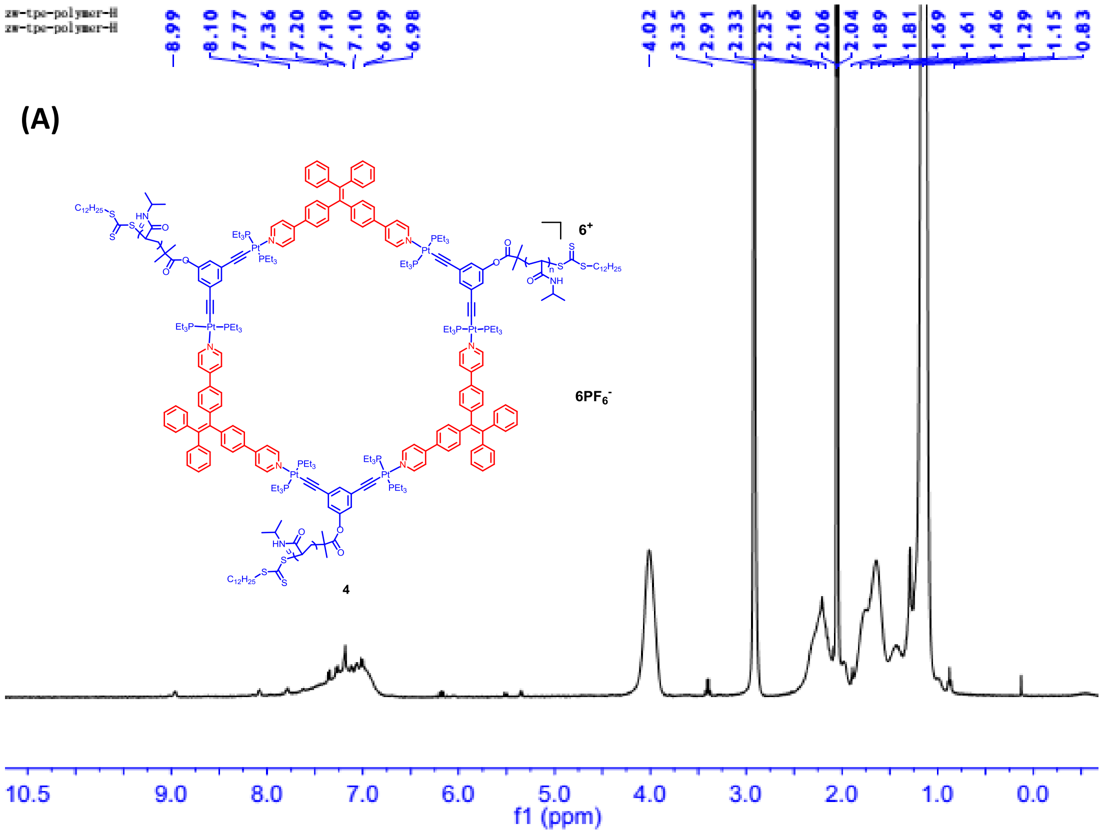

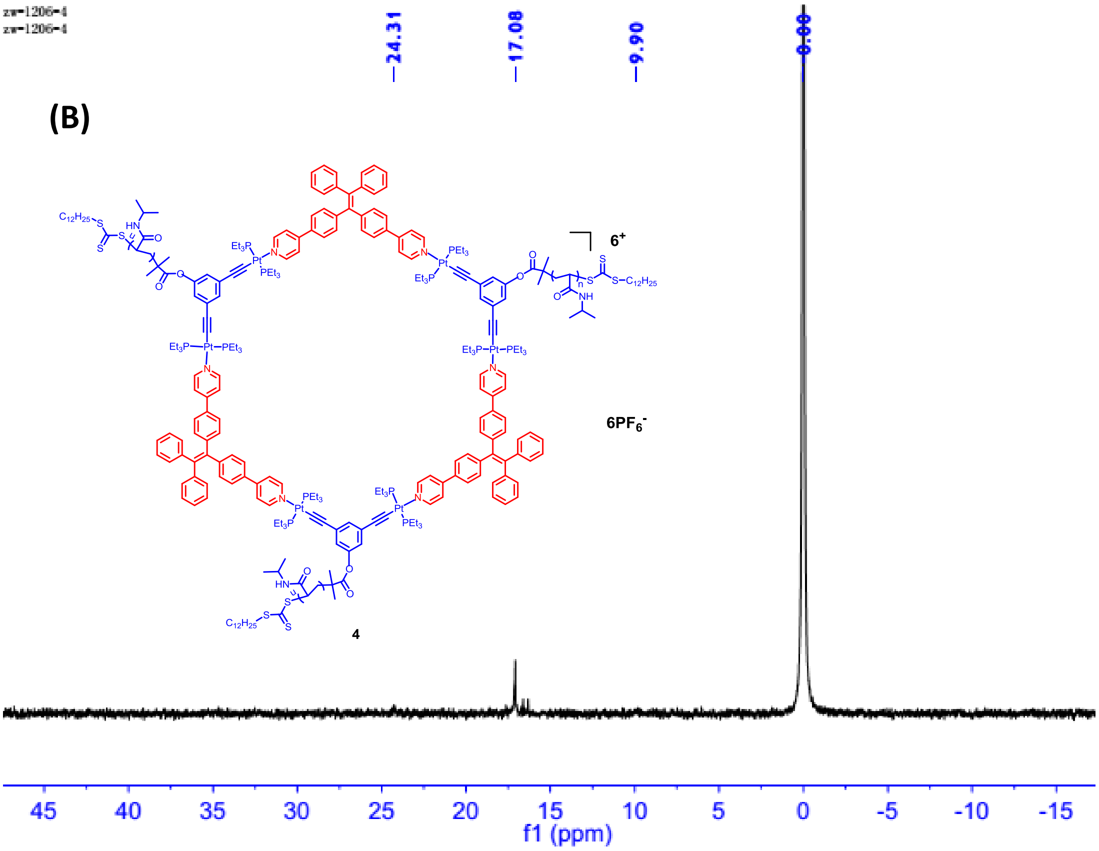

Fig. S11 (A) ^{1}H and (B) ^{31}P NMR spectra of polymer **4** in acetone-d_6.

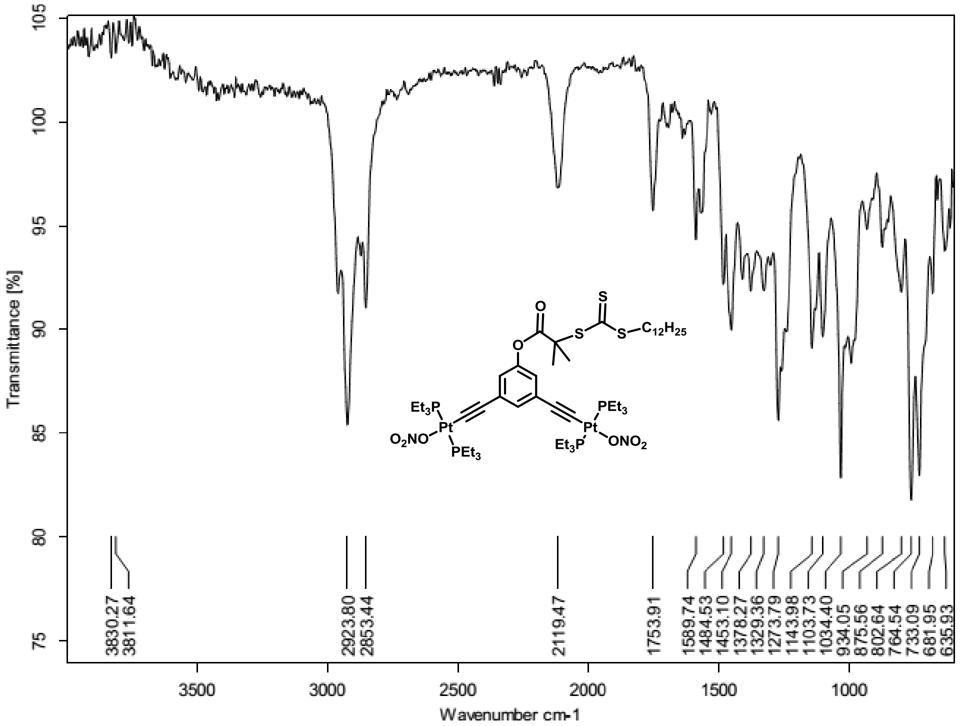

Fig. S12 IR spectrum of ligand **2**.

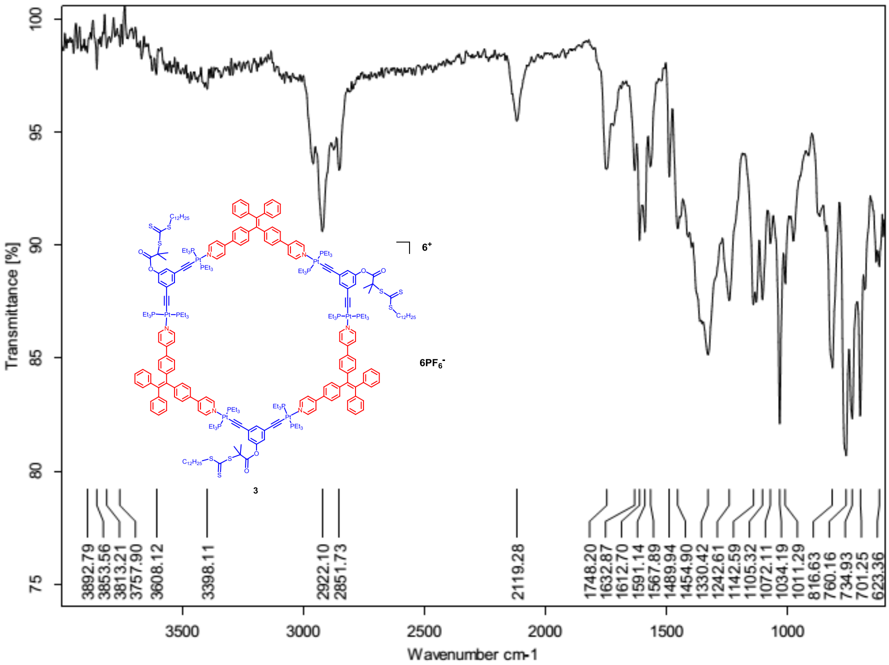

Fig. S13 IR spectrum of metallacycle **3**.

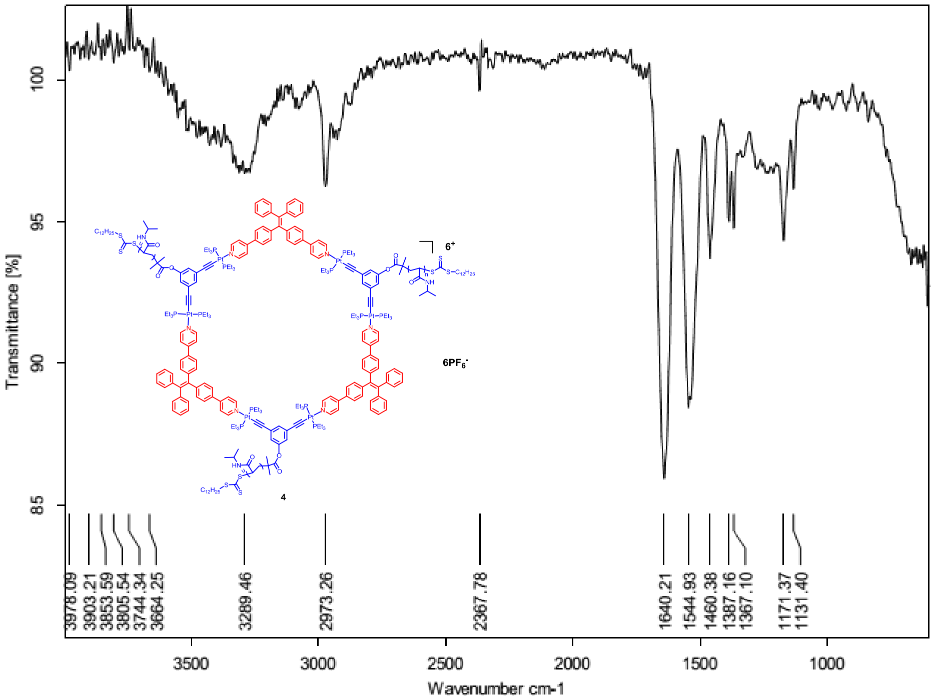

Fig. S14 IR spectrum of polymer **4**.

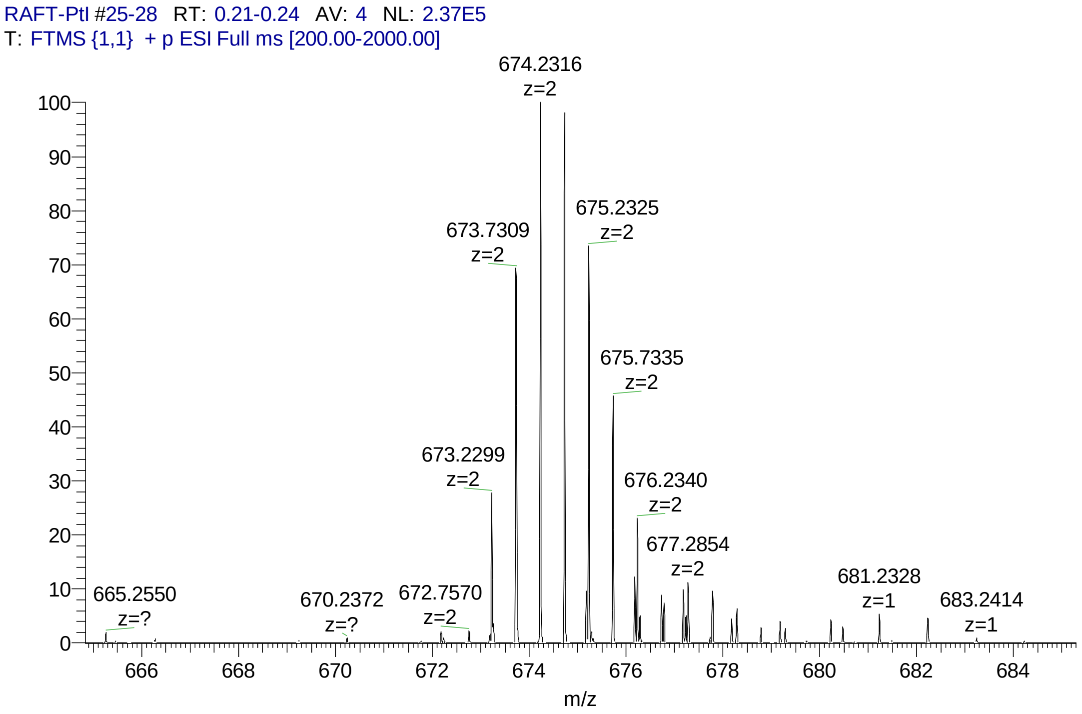

Fig. S15 ESI-MS spectrum of **c**.

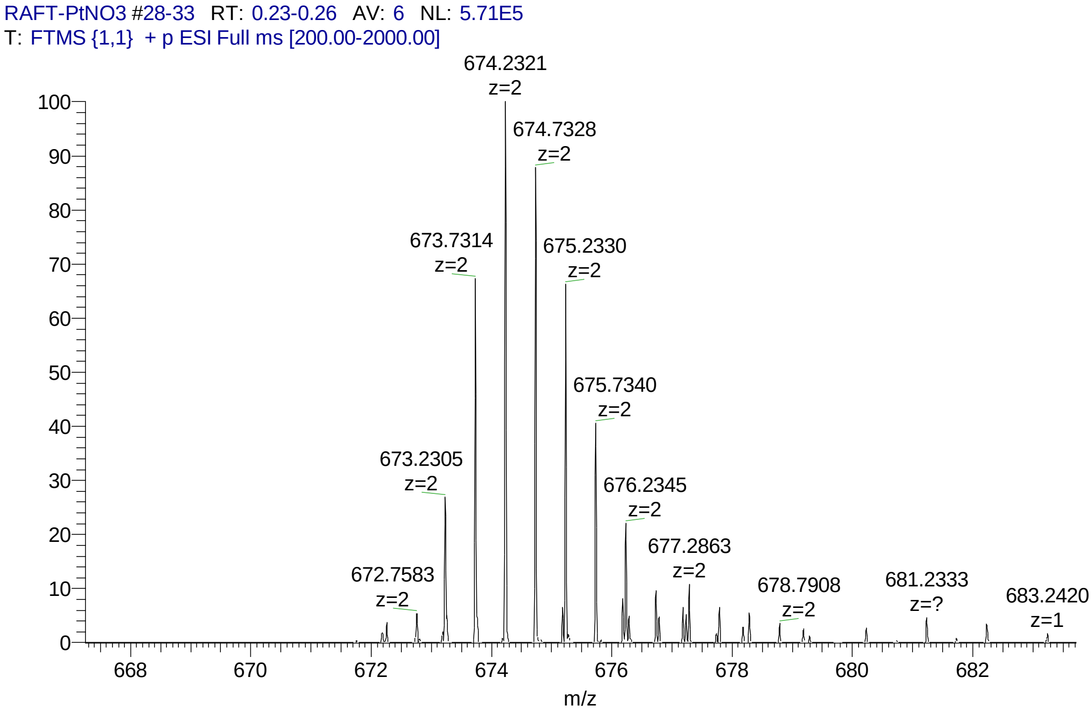

Fig. S16 ESI-MS spectrum of **2**.